



Short communication

High-performance poly(3,4-ethylene-dioxythiophene): polystyrenesulfonate conducting-polymer supercapacitor containing hetero-dimensional carbon additives



Yu-Ting Weng, Nae-Lih Wu*

Department of Chemical Engineering, National Taiwan University, Taipei 106, Taiwan, ROC

H I G H L I G H T S

- Electrode containing PEDOT (81%)/graphite oxide (16%)/CNT (3%) was studied.
- Composite electrode was prepared by facile solution casting method.
- Stacking of carbon additives leads to remarkable energy and power densities.
- Capacitance was increased from 85 F g⁻¹ to 365 F g⁻¹ by carbon addition.
- Composite electrode exhibits >100 Wh kg⁻¹-electrode at ca. 200 kW kg⁻¹.

A R T I C L E I N F O

Article history:

Received 7 December 2012

Received in revised form

10 March 2013

Accepted 15 March 2013

Available online 26 March 2013

Keywords:

Supercapacitor

Conducting polymer

Graphite oxide

Carbon nano-tube

A B S T R A C T

Supercapacitor composite electrode containing predominantly (81 wt.%) poly(3,4-ethylene-dioxythiophene):polystyrenesulfonate (PEDOT–PSS) conducting polymer (CP) and graphite oxide (GO; 16 wt.%) and carbon nanotube (CNT; 3 wt.%) has been prepared by a solution casting method. The stacking between these carbon additives having very different dimensionality provides a unique skeletal structure that allows for enlarged polymer/electrolyte interface for high-capacitance and for enhanced electronic and ionic conductivities needed for high-power performance. The resulting ternary electrode exhibits nearly ten-fold increase in energy and power performance as compared with pure CP electrode. It possesses a specific capacitance of 365 F g⁻¹-electrode over an operating potential window of 2.0 V, and exhibits a specific energy greater than 100 Wh kg⁻¹-electrode at the power of nearly 200 kW kg⁻¹-electrode with good cycle stability. Given the processing simplicity and outstanding power performance, the present PEDOT–PSSCP–C composite active material is considered possessing great potential for large-scale supercapacitor applications.

© 2013 Elsevier B.V. All rights reserved.

1. Introduction

Demand for electrochemical active materials in future electric-vehicle and renewable-energy storage applications is tremendous. For environmental concern, one clear challenge in the development of electrochemical energy storage cells would be to look for “greener” electrode materials having high abundance and low CO₂ footprints and being non-toxic. One solution to meet the goals is moving from inorganic to organic matter-based electrodes [1], which may be prepared from renewable resources (biomass) via processes that require lower processing temperatures than those for manufacturing inorganic materials. Conducting polymers

(CPs), possessing the potential of high electric conductivity and facile redox capability, are promising organic electrode materials for supercapacitor applications. Supercapacitors work based on two charge-storage mechanisms: surface ion adsorption (electric double layer capacitance, EDLC) and redox reactions (pseudocapacitance) [2]. Conducting polymers undergo redox reactions to store charge in bulk material and thereby increase the energy density and reduce self-discharge. Unfortunately, CP or CP-rich supercapacitors have so far exhibited insufficient power performance and short cycle life [3,4]. The former is partly due to slow diffusion of electrolyte ions within the bulk of the polymer matrix, while the latter originates primarily from failure of electrode structure caused by cyclic volumetric variations upon fast charge/discharge. Up to now, CP has found success in supercapacitor applications mainly as a secondary component, such as surface coating on EDLC materials

* Corresponding author. Tel.: +886 2 23627158; fax: +886 2 23623040.

E-mail address: NLW001@ntu.edu.tw (N.-L. Wu).

[5] and conductive binder in pseudocapacitive-oxide electrodes [6], in composite electrodes. In the case of surface coating on EDLC material, CP has typically been electrochemically plated from a monomer-containing solution onto EDLC electrode preforms [7]. Such a plating methodology is unfortunately incompatible with the roll-to-roll, large-scale electrode manufacturing processes.

Poly(3,4-ethylene-dioxythiophene):poly(styrenesulfonate) (PEDOT–PSS) is a polymer mixture of two ionomers. PEDOT is a *p*-type doped conjugated polymer, carrying positive charges, while the sulfonyl groups in PSS serve as “counter-ions” of PEDOT. PEDOT–PSS is commercially available in aqueous dispersion solution, which is suitable for thin-film formation. Owing to its very high conductivity, great ductility and processing simplicity, PEDOT–PSS has widely been used as conductive electrodes for flexible electronic and optoelectronic devices [8,9]. Nevertheless, PEDOT–PSS-rich supercapacitor electrodes have so far exhibited very limited capacitance ($<100 \text{ F g}^{-1}$) and limited power performance [10,11]. In this work, we demonstrate that introducing two carbon conductive additives with completely different dimensionalities, including two-dimensional graphite oxide (GO) flakes and one-dimensional multi-wall carbon nano-tube (CNT), into the PEDOT–PSS matrix can lead to remarkable (nearly 10 folds) enhancement in both energy and power performance of the polymer electrode, along with improved charge/discharge cycle stability. Given the processing simplicity and outstanding power performance, this PEDOT–PSS/CP-C composite active material is considered possessing great potential for large-scale supercapacitor applications.

2. Experimental

2.1. Preparation of PEDOT–PSS/GO/CNT composite films

Graphite oxide flakes were synthesized from graphite (Aldrich) following Brodie's method, while multi-wall CNT (Scientech Corporation; specific area $>380 \text{ m}^2 \text{ g}^{-1}$, diameter $<10 \text{ nm}$, length: $5\text{--}15 \mu\text{m}$) and PEDOT–PSS dispersion solution (Heraeus, PH1000) were used as purchased. PEDOT–PSS/GO/CNT composites electrode was fabricated from a mixture solution having weight ratios of PEDOT–PSS:GO:CNT = 0.81:0.16:0.03 in ethanol. The solution was stirred for 5 min twice with an intermittent sonication for 5 min. The mixed solution was then casted into continuous films on Ti foils, and then dried at 50°C for 30 min. Finally, the electrodes were dipped into ethylene glycol (EG) for 5 min, and then dried at 100°C for another 30 min. The other electrodes containing different C additives were prepared in the same manner except for different C types and/or contents. The electrode loading is ca. 0.3 mg .

2.2. Material and electrochemical characterizations

The electrodes were characterized by scanning electron microscopy (SEM; Nova NanoSEM 230; FEI Ultra-High Resolution FE-SEM), X-ray diffraction (XRD; Ultima IV, Rigaku) and Fourier Transform Infrared spectroscopy (ATR Spectrum 100, PerkinElmer). The Electrochemical properties of the electrodes were characterized by cyclic voltammetry (CV), galvanostatic charge/discharge, electrochemical impedance spectroscopy (EIS) on potentiostats (608, CH Instruments; Eco Chemie PGSTAT30, AUTOLAB). All of the experiments were carried out in three-electrode configuration which consists of the CP working electrode, a platinum foil counter electrode, and an Ag/AgCl/saturated KCl (EG&G, 197 mV versus NHE at 25°C) reference electrode. The electrolyte is 6 M NaNO_3 aqueous solution. Specific capacitance value (C) is calculated from cyclic voltammograms according to $C = \int I dt / m(dV/dt)$, with I being the current, dV/dt the scan rate, and m is the total mass of the active layer, including CP, C additive and binder, if any, in the working electrode.

3. Results and discussion

Fig. 1 compares the CV plots of different electrodes. The pristine PEDOT–PSS electrode (curve 1, Fig. 1a) exhibits two very different electrochemical behaviours between -1.0 V and 1.0 V . Above ca. -0.3 V , the plot exhibits a rectangular profile, typical of a capacitor, and an average specific capacitance of 85 F g^{-1} , which is similar to the literature values. In great contrast, the response current loop suddenly “pinches” as potential goes below -0.3 V . PEDOT is a *p*-type doped CP, and the capacitance reduction under negative polarization originates from reduced electronic conductivity due to loss in hole concentration. We expect to enlarge the operating potential window by introducing conductive additives, such as carbon nano-tube (CNT) and graphite, of which the conductivity would not be affected by potential polarization.

Mixing PEDOT–PSS either with CNT (3 wt.%) or graphite oxide (16 wt.%) can completely remove the “capacitance-pinching” phenomenon, and the lower operating potential limit is thus extended to -1.0 V (curves 2 and 3), beyond which reduction of water takes place. The operating potential window is therefore expanded from 1.3 V to nearly 2 V . This operating potential window is significantly greater than those ($0.8\text{--}1.0 \text{ V}$) of other CPs, including polypyrrole (Ppy) and polyaniline (PANI), that have often been suggested for supercapacitor electrodes.

One notes that the specific capacitance in the positive polarization region remains almost unchanged by addition of CNT. This suggests that the utilization of the CP component is not changed by the addition of 3 wt.% of CNT alone. Entanglement among the CNTs during electrode preparation becomes increasingly problematic as its content increases, leading to poor electrode morphology and deteriorated capacitance. In contrast, introducing the graphite oxide flakes upto 16 wt.% into the CP electrode has significantly enhanced the average specific capacitance to 195 F g^{-1} . The GO flakes apparently induce a greater effect in enhancing the utilization of the CP component than the CNTs. Although there is no practical content limit for GO, the electrode specific capacitance decreases with further increasing GO content due to insufficient conducting polymer component.

GO refers to graphite with oxidized surface [12]. XRD pattern (Fig. 2a) of the GO shows, in addition to the typical graphite basal-plane reflection with d -spacing of 0.34 nm , a small peak occurring at d -spacing of 0.70 nm . This small peak arises from expanded graphite basal planes, and its low intensity indicates that only a limited fraction, within the near surface region, of individual graphite flakes is expanded resulting from oxidation. FTIR analysis confirms the presence of abundant surface functional groups of OH and several oxygenated C species, including C=O , C-O-C and O-C-C . These surface functionalized graphite flakes can easily be blended into the CP dispersion solution at high contents ($>10 \text{ wt.}\%$) and show strong bonding with the CP.

The specific capacitance of GO is 11 F g^{-1} , while that of CNT is 23 F g^{-1} . Synergy in both capacitance and power performance takes place when the two carbon materials are simultaneously in presence. The electrode containing both GO (16 wt.%) and CNT (3 wt.%) exhibits a specific capacitance of 365 F g^{-1} (curve 4, Fig. 1a), maintaining a working potential range of nearly 2 V . Its specific capacitance is higher than that of either of the single-C additive electrodes as well as the sum of them. The charge-storage capacity is equivalent to ca. 200 mAh g^{-1} . As the contribution of either GO (curve 5) or CNT (curve 2) to the capacitance is negligible, the specific capacitance of the CP component in the ternary electrode therefore reaches 451 F g^{-1} -CP, which is quintuple that of the pristine CP (85 F g^{-1}). Furthermore, taking into account of the enhancements in both capacitance and working potential width,

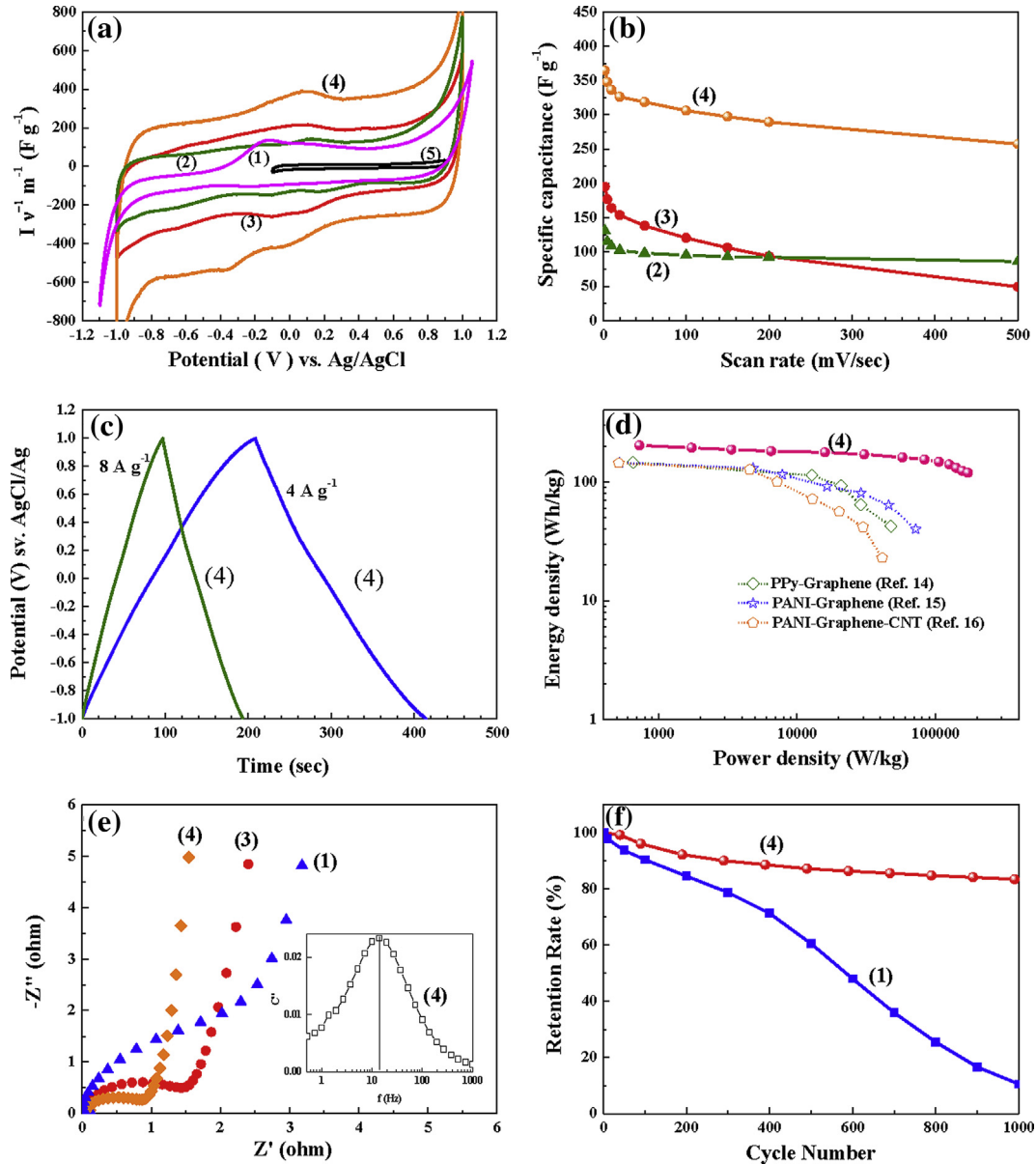


Fig. 1. Electrochemical characterizations: (a) cyclic voltammograms; (b) specific capacitance versus cycle scan-rate; (c) galvanostatic charge/discharge curves; (d) Ragone plots; (e) Nyquist plots; (f) capacitance retention versus cycle number. The number in parentheses indicates sample number: (1) pristine PEDOT–PSS; (2) PEDOT–PSS/CNT; (3) PEDOT–PSS/GO; (4) PEDOT–PSS/GO/CNT; (5) GO.

the specific energy of the electrode has been increased by nearly 10 folds (to 203 Wh kg^{-1}), as compared with the pristine CP electrode.

For power performance, as shown in Fig. 1b, the ternary composite electrode exhibits a specific capacitance of 255 F g^{-1} at the scan rate of 500 mV s^{-1} , corresponding to ca. 75% capacitance retention with a 250-fold increase in scan-rate (from 2 to 500 mV s^{-1}), and the capacitance is more than double that of either the CNT- (86 F g^{-1}) or the GO-added (50 F g^{-1}) electrode. Fig. 1c displays the galvanostatic charge/discharge potential curves of the ternary electrode. The potential curves exhibit linear potential–time relation from -1.0 to 1.0 V . The coulombic efficiency is greater than 99% in all cases. The average specific energy (E) and specific power (P) are calculated based on the following equations [13]:

$$E_{\text{electrode}} = \frac{1}{2} C (\Delta V)^2 \quad (1)$$

and

$$P_{\text{electrode}} = \frac{E}{t} \quad (2)$$

where C , ΔV and t are respectively specific capacitance, potential window (2.0 V), and discharge time (s). Fig. 1d shows the specific energy of single ternary electrode versus specific power. The specific energy reaches 206 Wh kg^{-1} at the low power level and maintains 138 Wh kg^{-1} even at the specific power of 192 kW kg^{-1} . In the same figure, we also compare recent literature data of a few graphene-based composite supercapacitor electrodes containing

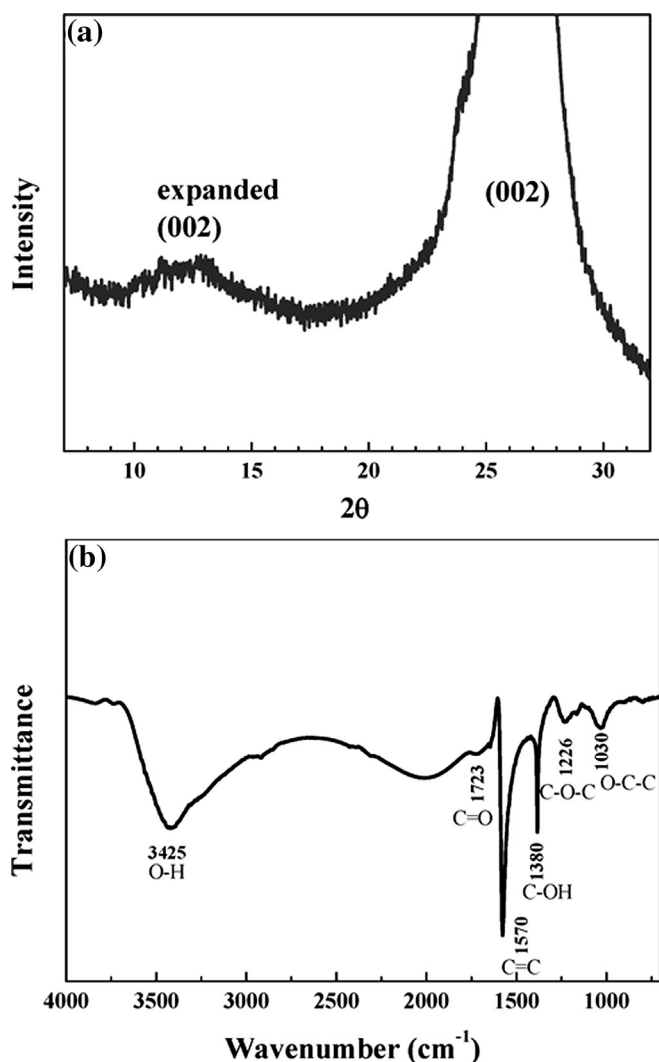


Fig. 2. (a) XRD and (b) FTIR spectra of GO.

different CPs, including PPy and PANI [14–16], for comparison. The present ternary electrode exhibits a much greater specific energy, particularly under high-powder conditions.

Fig. 1e compares the Nyquist plots of three electrodes with different C additive contents. All the plots show a (distorted) semi-circle in the medium frequency range. The diameter of the semi-circle approximately gives the overall resistance for electron transferring from the solid/electrolyte interface to current collector, including the redox charge-transfer resistance at the solid/electrode interface, electronic resistance through the electrode matrix and the electronic resistance at the active layer/current collector interface [17,18]. As shown, the semi-circle width is the largest for pristine PEDOT–PSS electrode, and it decreases upon introducing GO and further reduces with adding additional CNTs. The time constant determined from the peak-frequency of the imaginary capacitance plot (inset, Fig. 1e) of the ternary composite is 71 m s^{-1} . The time-constant determines the rate at which the electric response of the capacitor electrode can take place; the smaller the time-constant is, the faster the device can respond. The time-constant of the present ternary composite is at least one-order of magnitude smaller than those ($\sim 1 \text{ s}^{-1}$) typically reported in the literature for either activated carbon-based EDLC or CP and/or oxide-based pseudocapacitance supercapacitors [17,19,20]. Its small time constant echoes with its outstanding

power performance as shown in Fig. 1d. Finally, it is worth mentioning that the composite electrode exhibits much improved cycling stability (Fig. 1f). It retains greater than 80% capacitance after a thousand cycle under a current rate of 6 A g^{-1} , comparable to many oxide-based pseudocapacitors and far superior to pristine CP electrodes (Fig. 1f).

Coated by solution-casting followed by a simple heating process, the resulting PEDOT–PSS-rich electrodes do not exhibit structure failure, such as cracking or peeling, under high-angle bending, even in the cases of high C contents (Fig. 3a). This indicates good flexibility and the ability of the polymer to form strong adhesion to both metal current collector and the carbon components. SEM analysis shows the pristine CP electrode to be a smooth and dense film (Fig. 3b). The CNT-added electrode is also dense with CNTs embedded in the CP matrix (Fig. 3c). In contrast, the GO-added and GO–CNT-added electrodes show stacks of GO plates with randomly distributed macro-pores in between (Fig. 3d). These plates are apparently CP-coated GO flakes preferentially lying with their basal planes parallel to the electrode surface (Fig. 3e). The presence of the aligned GO flakes may enhance the bending strength of the active layer. The CP coating on GO is very uniform, as there is no voids or holes (bubbles) seen within the coating layer. These observations indicate very good interfacial compatibility between the CP and GO surface. As a result, the CP component also serves as an excellent binder to hold the C additives. In many cases, the side-view of the GO stacks in the ternary electrode reveals small gaps existing between the stacking GO plates (Fig. 3f). There is also observed streams of CNT extending between adjacent plates at different depths within the active layer.

The non-porous nature of the pristine and CNT-added CP electrodes render them having small specific capacitances, as only a small fraction of the CP is in contact with electrolyte. The occurrence of high density of macro-pores, which facilitates the penetration of electrolyte throughout the entire active layer, upon addition of GO flakes is the key to the significant increase in capacitance for both GO-added and the ternary electrodes. SEM analysis indicates that CNTs tend to be dispersed on the lateral planes of the GO plates. They may act as spacers between stacking GO flakes to form micro-/nano-pores/channels in between the plates. This is consistent with the frequent observation of the narrow “gaps” between GO plates in the ternary electrode (e.g., Fig. 3f). These pores and channels can enlarge the electrolyte/CP contact surface area, and provide fast diffusion pathways for electrolyte ions. Furthermore, the bulk conductivity of aligned graphite flakes can enhance in-plane electron transport within the active layer. The presence of the CNTs that run vertically through the electrode can help to enhance the out-of-plane conductivity of the entire electrode. The overall power performance is therefore enhanced with the presence of both carbon additives.

In conclusion, we demonstrate that introducing hetero-dimensional carbon additives, including GO and CNT, into the CP matrix leads to remarkable enhancement in both energy and power performance of the PEDOT–PSS supercapacitor electrode. The stacking between these carbon additives having very different dimensionality has provided a unique skeletal structure that allows for enlarged usage of the CP component for high-capacity and enhanced electronic and ionic conductivities needed for high-power operation. The resulting ternary electrode consisting of PEDOT–PSS/GO/CNT with the particular mass ratio of 81:16:3 possesses a specific capacitance of 365 F g^{-1} over an operating potential window of 2.0 V, and maintains a specific energy greater than 100 Wh kg^{-1} at the power of nearly 200 kW kg^{-1} with good cycle stability. To our knowledge, this is by far the highest specific energy ever reported at this power level for CP or CP-rich supercapacitor electrodes.

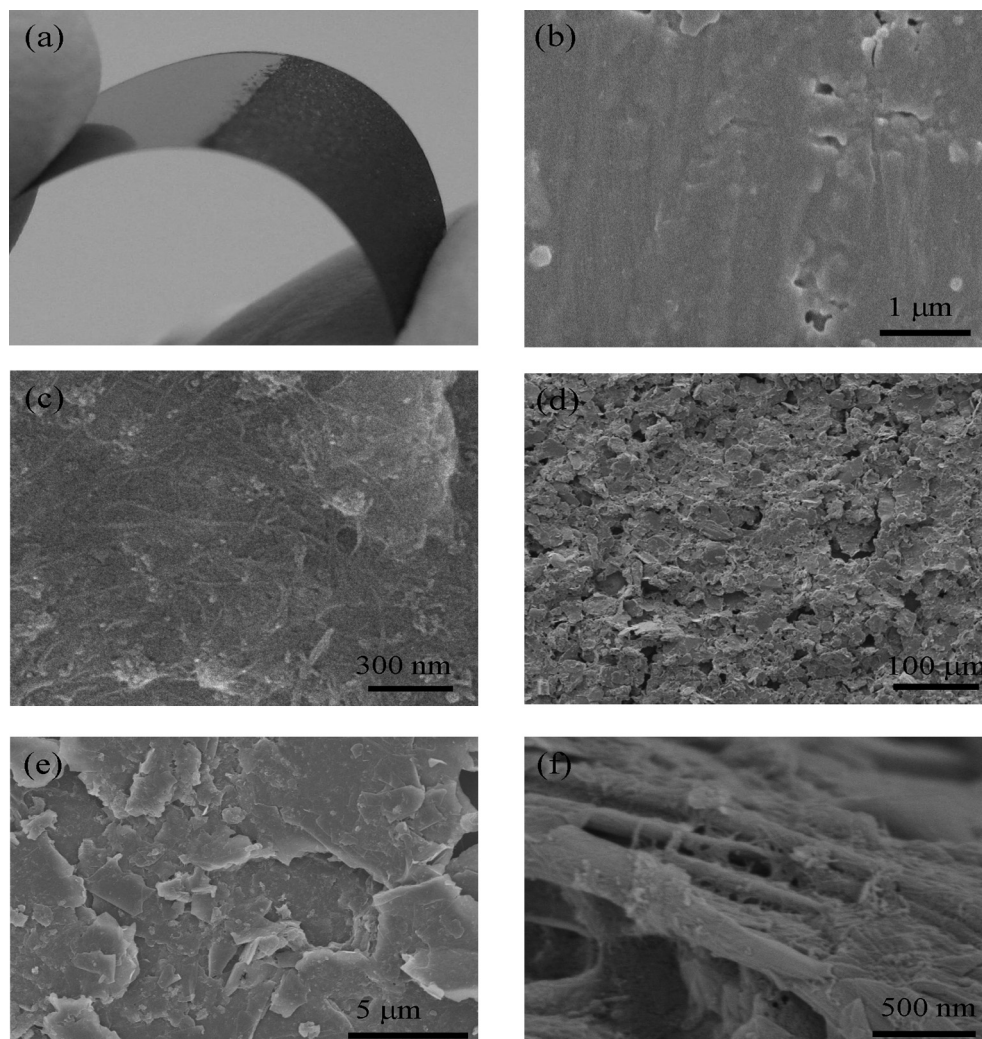


Fig. 3. Morphology and microstructures. (a) PEDOT–PSS/GO/CNT electrode under bending; (b) pristine PEDOT–PSS electrode; (c) PEDOT–PSS/CNT electrode; (d)–(f) PEDOT–PSS/GO/CNT electrode.

Acknowledgements

This work is partly supported by National Science Council, Taiwan (NSC 101-3113-E-006-010).

References

- [1] H. Chen, M. Armand, M. Courty, M. Jiang, C.P. Grey, F. Dolhem, J.M. Tarascon, P. Poizat, *J. Am. Chem. Soc.* 131 (2009) 8984–8988.
- [2] B.E. Conway, *J. Electrochem. Soc.* 138 (1991) 1539–1547.
- [3] Y. Zhang, H. Feng, X. Wu, L. Wang, A. Zhang, T. Xia, H. Dong, X. Li, L. Zhang, *Int. J. Hydrogen Energy* 34 (2009) 4889–4899.
- [4] G.A. Snook, P. Kao, A.S. Best, *J. Power Sources* 196 (2011) 1–12.
- [5] C. Peng, S. Zhang, D. Jewell, George Z. Chen, *Prog. Nat. Sci.* 18 (2008) 777–788.
- [6] L.M. Huang, H.Z. Lin, T.C. Wen, A. Gopalan, *Electrochim. Acta* 52 (2006) 1058–1063.
- [7] Y.R. Lin, H. Teng, *Carbon* 41 (2003) 2865–2871.
- [8] C.J. Brabec, C. Winder, N.S. Sariciftci, J.C. Hummelen, A. Dhanabalan, P.A. Hal, R.A.J. Janssen, *Adv. Funct. Mater.* 12 (2002) 709–712.
- [9] J. Ouyang, C.W. Chu, F.C. Chen, Q. Xu, Y. Yang, *Adv. Funct. Mater.* 15 (2005) 203–208.
- [10] S. Ghosh, O. Inganas, *Adv. Mater.* 11 (1999) 1214–1218.
- [11] F.J. Liu, *J. Power Sources* 182 (2008) 383–388.
- [12] T. Szabó, O. Berkesi, P. Forgó, K. Josepovits, Y. Sanakis, D. Petridis, I. Dékány, *Chem. Mater.* 18 (2006) 2740–2749.
- [13] Q. Wu, Y. Xu, Z. Yao, A. Liu, G. Shi, *ACS Nano* 4 (2010) 1963–1970.
- [14] S. Bose, N.H. Kim, T. Kuila, K.T. Lau, J.H. Lee, *Nanotechnology* 22 (2011) 295202–295211.
- [15] J. Yan, T. Wei, B. Shao, Z. Fan, W. Qian, M. Zhang, F. Wei, *Carbon* 48 (2010) 487–493.
- [16] J. Yan, T. Wei, Z. Fan, W. Qian, M. Zhang, X. Shen, F. Wei, *J. Power Sources* 195 (2010) 3041–3045.
- [17] P.L. Taberna, P. Simon, J.F. Fauvarque, *J. Electrochem. Soc.* 150 (2003) A292–A300.
- [18] J.-M. Atebamba, J. Moskon, S. Pejovnik, M. Gaberscka, *J. Electrochem. Soc.* 157 (2010) 1218–1228.
- [19] Y. Kou, Y. Xu, Z. Guo, D. Jiang, *Angew. Chem. Int. Ed.* 50 (2011) 8753–8757.
- [20] J.H. Jang, A. Kato, K. Machida, K. Naoi, *J. Electrochem. Soc.* 153 (2006) A321–A328.